ACS APPLIED NANO MATERIALS

www.acsanm.org Article

Si/Au Hybrid Nanoparticles with Highly Efficient Nonlinear Optical Emission: Implication for Nanoscale White Light Sources

Xiaobing He, ShiMei Liu, Shulei Li, Mingcheng Panmai, and Sheng Lan*

Cite This: *ACS Appl. Nano Mater.* 2022, 5, 10676−10685 Read Online

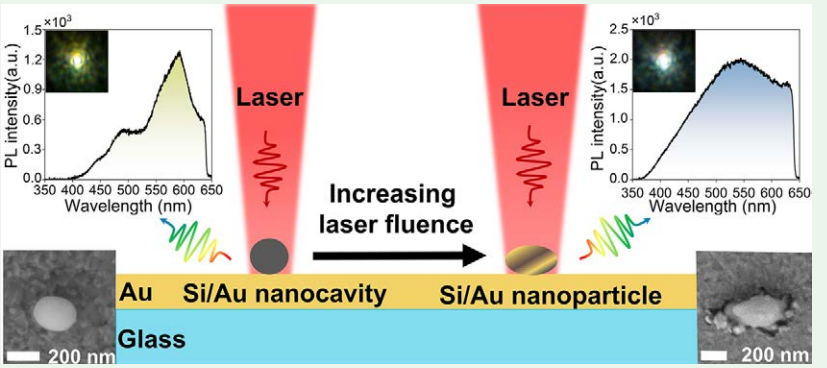

ABSTRACT: Nanoscale white light sources are being pursued for many practical applications such as spectroscopy and imaging. Here, we proposed a simple method for fabricating Si/Au hybrid nanoparticles and demonstrated highly efficient white light emission from such nanoparticles. We fabricated Si nanoparticles by using femtosecond laser ablation and constructed Si/Au nanocavities by placing Si nanoparticles on a thin Au film. We excited Si/Au nanocavities with femtosecond laser pulses and observed the burst of hot electron luminescence from such nanocavities. It was found that Si/Au hybrid nanoparticles can be obtained by intentionally irradiating Si/Au nanocavities with a large excitation irradiance (or laser fluence). Burst of hot electron luminescence was also observed in Si/Au hybrid nanoparticles. Efficient and stable white light emission with a quantum efficiency of ∼1.0% could be achieved above the threshold. The luminescence lifetime of Si/Au hybrid nanoparticles was found to be ∼1.00 ns, which is much longer than that observed for Si/Au nanocavities. Our findings are helpful for understanding the nonlinear optical emission from semiconductor−metal hybrid nanostructures and useful for designing nanoscale white light sources for practical applications.

KEYWORDS: *Si nanoparticle, femtosecond laser ablation, Si/Au nanocavity, Si/Au hybrid nanoparticle, white light emission*

1. INTRODUCTION

Nanoscale broadband light sources with high quantum efficiencies, which can be employed for probing the near fields and density of states of nanophotonic devices, are highly desirable in advanced spectroscopy.[1−3] So far, it has been found that many kinds of nanomaterials can emit broadband photoluminescence (PL) under the excitation of pulsed laser light, including noble metals[4−9] and semiconductors.[10−12] For metallic thin films or nanoparticles, broadband PL is generated by femtosecond laser pulses originating from the intraband transition of hot electrons.[13,14] In this case, the PL from plasmonic hot spots resembles the radiation of a blackbody.[15−17] The peak position is blueshifted with increasing excitation irradiance or electron temperature. Consequently, the slope derived from the dependence of the luminescence intensity on the excitation irradiance exhibits a linear relationship with the energy of the emitted photon.[18]

In addition to metallic nanoparticles, broadband PL was also discovered in semiconductor nanoparticles supporting Mie resonances, such as GaAs and Si nanoparticles. For GaAs nanoparticles, the broadband PL arises from the intraband transition of hot electrons, which is similar to metallic nanoparticles.[11] In contrast, the broadband PL of Si nanoparticles is ascribed to the interband transition of hot electrons assisted by phonons.[10,12] It was realized early that the PL from a semiconductor nanomaterial can be improved by using a thin metal film. Lasing action was achieved in a CdS nanowire

Received: May 6, 2022
Accepted: July 14, 2022
Published: July 25, 2022

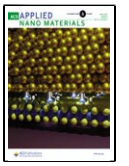

https://doi.org/10.1021/acsanm.2c01982
ACS Appl. Nano Mater. 2022, 5, 10676−10685

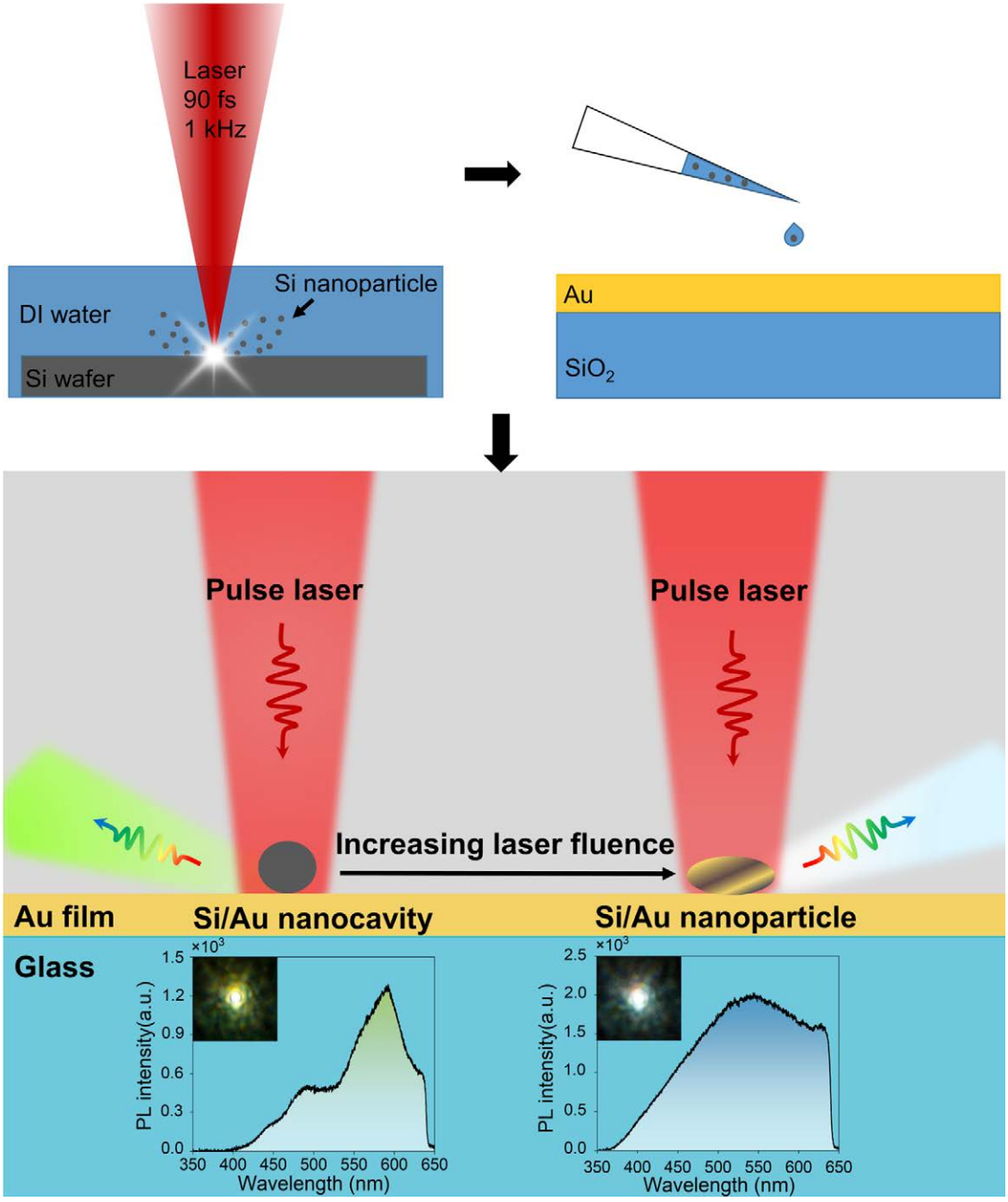

Figure 1. Schematic showing the fabrication of Si/Au hybrid nanoparticles by irradiating Si/Au nanocavity with femtosecond laser light. Also shown are the white light emissions (CCD images) and PL spectra of a Si/Au nanocavity (left) and a Si/Au nanoparticle (right).

placed on a thin Ag film by utilizing the gap mode formed in between the CdS nanowire and the Ag film.[19,20] For Si nanomaterials with an indirect band gap, it was shown that the hot electron luminescence from a Si nanowire can be significantly boosted by exploiting the Purcell effect[21] induced by a thin silver (Ag) film surrounding the Si nanowire.[22,23] In this case, the hot electron luminescence originates from the interband transition of hot electrons assisted by phonons.[22,24] In addition, it was found that the PL from a Si nanoparticle can be dramatically enhanced by placing the Si nanoparticle on a thin sliver (Ag) film, creating a Si/Ag nanocavity.[25] In this case, the mirror-image-induced magnetic dipole[26,27] (MMD) supported by the Si/Ag nanocavity is employed to increase significantly the nonlinear optical absorption of the Si nanoparticle, providing a higher quantum efficiency and a lower threshold for the luminescence burst.[25] It was found that the Si nanoparticle can be heated to a temperature as high as ∼1600 K and the intrinsic transition of carrier leads to the luminescence burst of the Si nanoparticle.

Although stable white light emission from a Si/Ag nanocavity was confirmed for an excitation irradiance slightly above the threshold, a further increase in the excitation irradiance will lead to the damage of the Si/Ag nanocavity. Recently, it was found that efficient broadband PL could be achieved in Si/Au hybrid nanoparticles prepared by using femtosecond laser ablation.[28−31] Therefore, it is interesting to know whether Si/Au hybrid nanoparticles with efficient white light emission can be obtained by simply irradiating a Si/Au

https://doi.org/10.1021/acsanm.2c01982
ACS Appl. Nano Mater. 2022, 5, 10676−10685

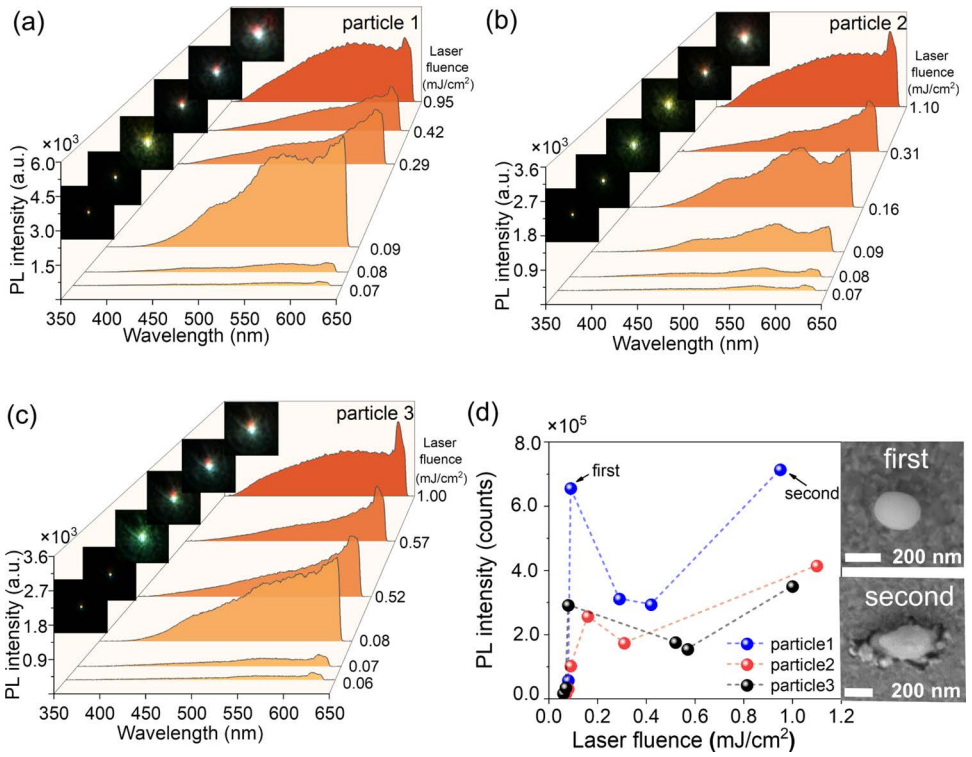

Figure 2. (a–c) Evolutions of the PL spectrum and CCD image with increasing excitation irradiance observed for three Si/Au nanocavities. (d) Dependence of the PL intensity on the excitation irradiance observed for three Si/Au nanocavities. The SEM images for the Si nanoparticle after the first luminescence burst and the Si/Au nanoparticle after the second luminescence burst are shown in the insets.

nanocavity with an excitation irradiance above the threshold for luminescence burst. In addition, it is important to compare the optical properties of Si/Au hybrid nanoparticles with those of Si/Au nanocavities.

Apart from Si/Au hybrid nanoparticles fabricated by femtosecond laser ablation, there are many other methods for preparing hybrid nanoparticles with various practical applications. For example, Ag nanoparticles embedded in lithium niobate were synthesized by ion implantation and such hybrid nanoparticles were employed as efficient broadband saturable absorber to realize a Q-switched pulse laser.[32] In addition, silica (SiO_2) nanoparticles with Au nanoshells were produced with a seeded-growth method and SiO_2/Au nanocups were fabricated by depositing Au layers on SiO_2 nanoparticles.[33] Such hybrid nanoparticles were successfully applied in the highly efficient second harmonic generation.[34] Snowman-like Janus particles were fabricated by seed emulsion polymerization, and they exhibit excellent catalytic performance.[35] Therefore, the hybrid Si/Au hybrid nanoparticles investigated in this work are expected to exhibit potential applications in harmonic generation, saturable absorber, and catalysts. In this work, we focus mainly on the nonlinear optical emission of Si/Au hybrid nanoparticles and their application in nanoscale white light source.

2. RESULTS AND DISCUSSION

In Figure 1, we show schematically a Si/Au nanocavity created by placing a Si nanoparticle on a 50-nm-thick Au film and the transformation of the Si/Au nanocavity into a Si/Au hybrid nanoparticle induced by laser irradiation. In this case, the Si/Au nanocavity is excited by 720-nm femtosecond laser pulses and the increase of the excitation irradiance (or laser fluence) above a threshold lead to the formation of the Si/Au hybrid nanoparticle. Here, we also show the PL spectra measured for the Si/Au nanocavity and the Si/Au nanoparticle. Their emission images taken by a charge-coupled device (CCD) are also shown in the insets. Compared with the Si/Au nanocavity, the PL spectrum of the Si/Au nanoparticle is apparently changed. The two peaks located at ~480 and ~575 nm in the PL spectrum of the Si/Au nanocavity, originating from the enhancements at the optical resonances supported by the nanocavity, disappear completely in the PL spectrum of the Si/Au nanoparticle. Accordingly, the color of the PL is also changed from green to white, as manifested in the CCD images.

Now we examine the evolutions of the PL spectrum and CCD image of several Si/Au nanocavities with increasing laser fluence, as shown in Figure 2a–c. In order to show clearly the change in the luminescence spectrum, we present typical luminescence spectra at specific laser fluences for different Si/Au nanocavities. These Si/Au nanocavities support optical resonances at ~720 nm, which are usually referred to as MMD (see Figure 3 for a typical case).[26,27] Physically, each MMD mode originates from the interference of the electric dipole (ED) supported by the Si nanoparticle and its mirror image induced by the Au film. Basically, the resonant wavelength of the MMD mode is determined by the diameter of the Si nanoparticle used to construct the Si/Au nanocavity. Since Si nanoparticles used to construct Si/Au nanocavities were prepared by femtosecond laser ablation, the difference in the diameter of the Si nanoparticle may result in the difference in the resonant wavelength of the MMD mode. The nonlinear optical absorption of the Si nanoparticle can be greatly enhanced when the MMD mode is resonantly excited by using femtosecond laser pulses. In our case, we used 720-nm femtosecond laser pulses to excite Si/Au nanocavities with

https://doi.org/10.1021/acsanm.2c01982
ACS Appl. Nano Mater. 2022, 5, 10676–10685

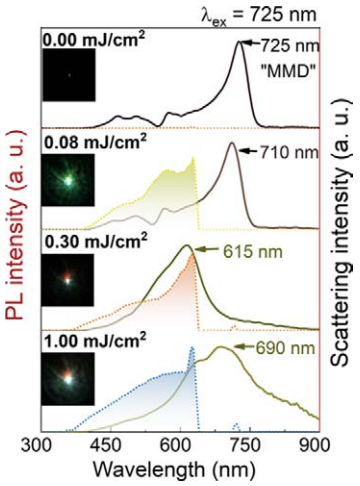

Figure 3. Scattering spectra measured for a Si/Au nanocavity after being irradiated by using femtosecond laser light with different fluences (solid curves). Also shown are the PL spectra of the Si/Au nanocavity (shaded area) and the CCD images of the hot electron luminescence.

MMD modes located at ~720 nm. The upconverted PL at the short-wavelength side of the MMD mode (λ < 630 nm) was detected. The excitation laser light is removed by using a high-pass optical filter inserted in the signal collection channel. In Figure 2a–c, one can observe luminescence burst twice. The first one appears at a laser fluence of ~0.08 mJ/cm^2. The thresholds for the luminescence burst are slightly different for the three Si/Au nanocavities owing to the small difference in the resonant wavelength of the MMD mode. The physical mechanism for the luminescence burst of a Si/Au nanocavity has been discussed in detail in our previous study.[25] The carrier dynamics in the Si nanoparticle is modified by injecting high-density carriers into the Si nanoparticle via the nonlinear optical absorption, which is significantly enhanced at the MMD mode. The relaxation time (nonradiative lifetime) is greatly increased by the Auger recombination process, while the radiative lifetime is dramatically shortened, resulting in quantum efficiency enhanced by several orders of magnitude. On the other hand, the high temperature induced by the thermalization of hot electrons will trigger the intrinsic excitation of carriers, supplying continuously carriers to the Δ point of the conduction band and accelerating the Auger recombination process. The cooperation of these two mechanisms leads to the luminescence burst observed for the Si/Au nanocavity when the laser fluence exceeds a critical value.

The thresholds for the luminescence burst are slightly different for the three Si/Au nanocavities owing to the small difference in the resonant wavelength of the MMD mode. In this case, the Si nanoparticle in the Si/Au nanocavity is lighted up and the PL is enhanced at other optical resonances supported by the Si/Au nanocavity. As a result, the emission from the nanocavity does not appear as white light, as shown in the CCD images, especially for the third Si/Au nanocavity whose PL appears as green light. However, a reduction in PL is observed when we increase the laser fluence. In this case, it is thought that the Si/Au nanocavity is damaged by high temperature, which leads to the melting of the Si nanoparticle and the Au film. Surprisingly, the second luminescence burst is observed when the laser fluence is raised to ~1.0 mJ/cm^2. It is noticed that the enhancement appearing at the short-wavelength side of the spectrum disappears completely. As a result, the PL appears as white light. In addition, it becomes more stable against the increase of the laser fluence. In Figure 2d, we present the dependence of the luminescence intensity on the laser fluence measured for the three Si nanoparticles (including Si/Au nanocavities and Si/Au nanoparticles). One can clearly identify the thresholds for the two luminescence bursts. While the first luminescence burst appears abruptly, the second one occurs gradually.

It is thought that the white light emission after the second luminescence burst arises from Si/Au hybrid nanoparticles formed by Si and Au nanoparticles with smaller sizes. To confirm this, we examined the scattering spectrum of the Si nanoparticle at different laser fluences, as shown in Figure 3. The corresponding PL spectrum and CCD images are also provided for reference. It is remarkable that the MMD mode supported by the Si/Au nanocavity, which appears at ~725 nm at the initial stage, is blueshifted to ~710 nm when the first luminescence burst occurs at ~0.08 mJ/cm^2. Apart from the slight blueshift of the MMD mode, the scattering spectrum remains almost unchanged. When the laser fluence is increased to 0.30 mJ/cm^2, a reduction of the PL is observed. In addition, the scattering peak is blueshifted to ~615 nm and broadened. As the laser fluence was further increased to 1.00 mJ/cm^2, a rapid increase in the PL was found. Moreover, the scattering peak is redshifted to ~690 nm and broadened again.

To obtain a deep insight into the formation of Si/Au hybrid nanoparticles, we examined morphologies of Si/Au nanocavities after the first and second luminescence burst by using scanning electron microscopy (SEM). A typical example is shown in Figure 4. After the first luminescence burst, the Si nanoparticle was elongated to some extent along the polarization of the laser light. This morphological change from a sphere to an ellipsoid is responsible for the blueshift of the MMD mode observed in Figure 3. After the second luminescence burst, it is found that the Si nanoparticle and the

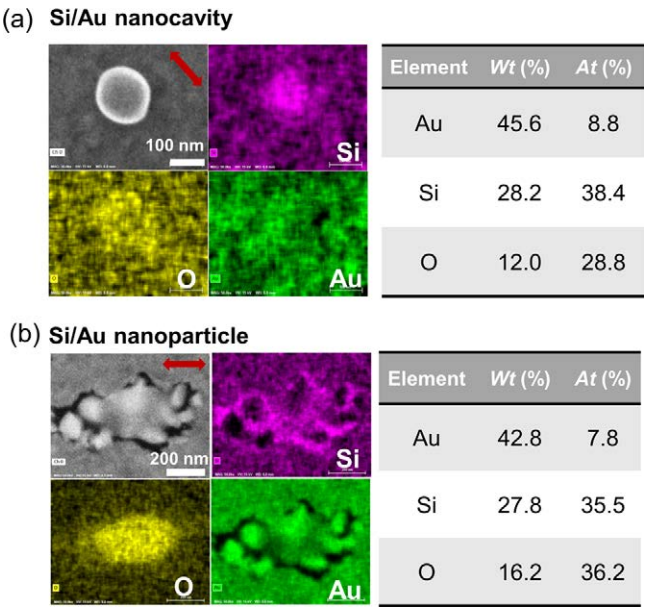

Figure 4. EDS analysis performed for (a) Si/Au nanocavity and (b) Si/Au nanoparticle (laser polarization direction is shown by a red arrow).

https://doi.org/10.1021/acsanm.2c01982
ACS Appl. Nano Mater. 2022, 5, 10676–10685

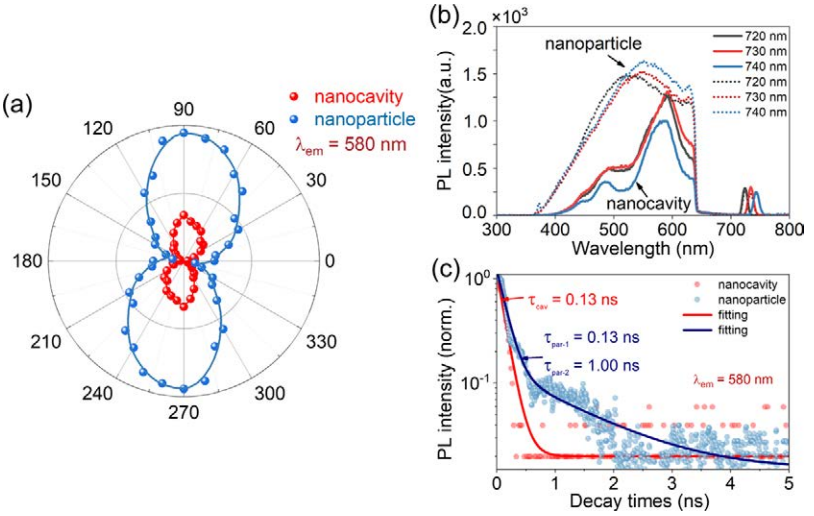

Figure 5. (a) Dependence of the luminescence intensity on the polarization angle of the polarization analyzer measured for a Si/Au nanocavity and a Si/Au nanoparticle at λ_{em} = 580 nm. (b) PL spectra measured for Si/Au nanocavities (solid curves) and Si/Au nanoparticles (dashed curves) at different excitation wavelengths. (c) Luminescence decay measured for a Si/Au nanocavity (red dots) and a Si/Au nanoparticle (blue dots) at λ_{em} = 580 nm. Also shown are the single- and biexponential fittings of the luminescence decays from which the lifetimes are extracted.

Au film are completely damaged by high temperature, forming a Si/Au hybrid nanoparticle with an irregular shape. The formation of the Si/Au hybrid nanoparticle is confirmed by energy-dispersive spectroscopy (EDS), as shown in Figure 4. From the SEM image and the EDS analysis, the internal morphology of a Si/Au hybrid nanoparticle is still not very clear. Previously, similar Si/Au nanoparticles were obtained by using femtosecond laser ablation.[1] The internal morphology of such a Si/Au nanoparticle was revealed by using transmission electron microscopy (TEM). In our case, the as-prepared Si/Au hybrid nanoparticles were located on a thin Au film, making it difficult to determine their internal morphologies by using TEM observation. However, we think that the internal morphologies of Si/Au hybrid nanoparticles are similar to those reported in previous literature.[1] It means that a Si/Au nanoparticle is composed of Si and Au nanoparticles with much smaller sizes. The localized electric field around Au nanoparticles enhances the nonlinear optical absorption of Si nanoparticles while the nonlinear optical emission comes from both Si and Au nanoparticles.

We examined the polarization of the PL emitted from a Si/Au nanocavity and a Si/Au nanoparticle by inserting a polarization analyzer in the signal collection channel. The dependences of the PL intensity on the polarization angle obtained for the Si/Au nanocavity and the Si/Au nanoparticle are shown Figure 5a. In both cases, linearly polarized PL is obtained. We also compared the PL spectra of Si/Au nanocavity and Si/Au nanoparticle measured by using femtosecond laser pulses at different wavelengths, as shown in Figure 5b. It is noticed that the PL intensity of the Si/Au nanoparticle is not sensitive to the excitation wavelength while a redshift of the PL peak is discovered with increasing excitation wavelength. In comparison, a reduction in the PL intensity is observed for the Si/Au nanocavity with increasing excitation wavelength. Moreover, the PL spectrum of the Si/Au nanocavity remains nearly unchanged when the excitation wavelength is varied. It is thought that the PL from the Si/Au nanocavity originates from the interband transition of hot electrons in the Si nanoparticle while that from the Si/Au nanoparticle arises from the intraband transition of hot electrons in Au nanoparticles. Since the bandgap energy of Si at the Γ point is ∼3.4 eV, the electrons in the valance band can be vertically lifted to the conduction band by using single-photon excitation at ∼360 nm and two-photon excitation at ∼720 nm. It implies that a higher carrier density will be obtained when the excitation wavelength approaches ∼720 nm. For a Si/Au nanoparticle, the nonlinear optical emission comes from both Si and Au nanoparticles. Previously, it was found that the hot electron luminescence from the plasmonic hot spots on a rough Au film is blueshifted with increasing excitation intensity (or carrier density).[18] Therefore, we think that the reduction in the carrier density with increasing excitation wavelength from 720 to 740 nm is responsible for the redshift of the PL peak. We also compared the luminescence decays of Si/Au nanocavities and Si/Au nanoparticles, as shown in Figure 5c. It is noticed that the luminescence of the Si/Au nanocavity exhibits a single exponential decay with a time constant of ∼0.13 ns. In contrast, biexponential decay with time constants of ∼0.13 and ∼1.00 ns is observed for the Si/Au nanoparticle. Similar to the previous study on Si/Au nanoparticles,[1] we attributed the fast decay to the PL from Si/Au nanoparticles and the slow one to the defect-assisted processes.

In general, the external quantum efficiency for the PL of a semiconductor material (η) can be expressed as follows:

$$\eta = \frac{N^{em}}{N^{in}} \tag{1}$$

where N^{in} and N^{em} denote the number of electron−hole pairs injected into the material and the number of photons emitted out of the material. For the nonlinear optical emission or upconverted PL generated via a two-photon-induced absorption (TPA) process, the external quantum efficiency can be written as:

$$\eta = 2\frac{N^{em}}{N^{abs}} \tag{2}$$

where $N^{abs} = 2N^{in}$ is the number of photons absorbed by the material via the TPA process because the absorption of two photons leads to the generation of one electron−hole pair.

https://doi.org/10.1021/acsanm.2c01982
ACS Appl. Nano Mater. 2022, 5, 10676−10685

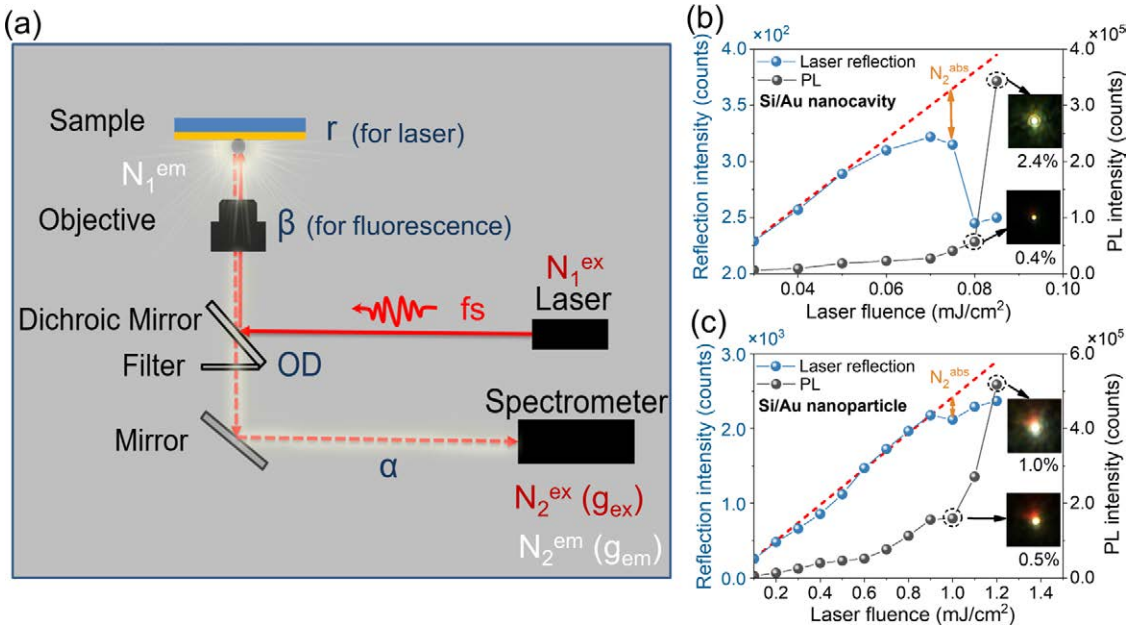

Figure 6. (a) Experimental setup used to evaluate the quantum efficiencies of Si/Au nanocavities and Si/Au nanoparticles. (b,c) Dependences of the reflected laser light intensities from the substrate without and with Si or Si/Au nanoparticles on the laser fluence (blue dots). The dependence of the luminescence intensity on the laser fluence is also provided for reference (black dots). The CCD images of the luminescence below and above the threshold are shown in the insets.

In practice, measuring the external quantum efficiency of a nanoparticle still faces great challenges. Here, we estimated the external quantum efficiency for a Si/Au nanocavity or a Si/Au nanoparticle based on the method proposed by us in previous studies.[12,25] As schematically shown in Figure 6a, the excitation laser beam was directed to the objective of a microscope by a dichroic mirror and focused on the Si nanoparticle. The PL coming from the Si nanoparticle is gathered by the same objective and sent to the spectrometer for spectral analysis. Meanwhile, a fraction of the excitation light reflected from the substrate is also delivered to the spectrometer after passing through a high-pass filter. At low laser fluences, the intensity of the reflected laser light is proportional to that of the excitation laser light. However, a deviation from the linear relationship is observed at high laser fluences when the nonlinear optical absorption becomes dominant over the linear one. Consequently, the nonlinear optical absorption of the Si/Au nanoparticle (i.e., N^{abs}) can be derived. In addition, the number of photons emitted from the nanoparticle (i.e., N^{em}) can be estimated when the optical loss of the measurement system is known.

As depicted in Figure 6a, a part of the excitation laser light focusing on the Si nanoparticle will be reflected by the Si nanoparticle on the substrate. The reflected laser light will pass the dichroic mirror and a high-pass filter with an optical density (OD) of $\sim 2.3 \times 10^{-6}$ before reaching the spectrometer.[25] The total number of photons detected by the CCD, that is, N_2^{ex}, can be expressed as follows:

$$N_2^{ex} = N_1^{ex} \cdot r \cdot \mathrm{OD} \cdot \alpha \cdot g_{ex} \cdot \eta_{ex} \tag{3}$$

where N_1^{ex} is the total number of photons shining on the Si nanoparticle and the substrate, r is the corresponding reflectivity, α is the attenuation coefficient of the optical system (except the dichroic mirror and the optical filter), g_{ex} and η_{ex} are the gain and quantum efficiency of the CCD. Therefore, the number of photons absorbed by the Si nanoparticles (N_1^{abs}) via the TPA processes can derived from the reduction in the reflected laser light (N_2^{abs}):

$$N_2^{abs} = N_1^{abs} \cdot r \cdot \mathrm{OD} \cdot \alpha \cdot g_{ex} \cdot \eta_{ex} \tag{4}$$

Similarly, we can obtain the similar relationship between the number of photons (N_2^{em}) detected by the spectrometer and the number of photons emitted from the Si nanoparticle (N_1^{em}):

$$N_2^{em} = N_1^{em} \cdot \beta \cdot \alpha \cdot g_{em} \cdot \eta_{em} \tag{5}$$

where the collection efficiency of the objective lens (β), which is influenced by the substrate, is taken into account. For Si nanoparticles located on an Au/SiO_2 substrate, we obtained an average collection efficiency of $\beta \sim 0.52$ in the visible to near infrared spectral range based on numerical simulation.

Having known the number of photons absorbed by the Si nanoparticle (N_1^{abs}) and that emitted from the Si nanoparticle (N_1^{em}), one can derive the external quantum efficiency for the hot electron luminescence of a Si/Au nanocavity or a Si/Au nanoparticle, which is given as follows:

$$Q = 2\frac{N_1^{em}}{N_1^{abs}} = 2\frac{N_2^{em} \cdot r \cdot \mathrm{OD} \cdot \eta_{ex}}{N_2^{abs} \cdot \beta \cdot \eta_{em}} \tag{6}$$

Based on the linear relationship between the reflected laser light intensity and the laser fluence shown in Figure 6b,c, we can derive the attenuation coefficient α of the measurement system. In this case, the number of photons containing in the excitation laser light (N_1^{ex}) and that detected by the CCD (N_2^{ex}) is related by eq 3. For a laser fluence of 0.04 mJ/cm^2 and a laser spot diameter of 2.0 μm, we have

$$N_1^{ex} = \frac{w \cdot s}{h\nu} = \frac{0.04\ \mathrm{mJ/cm^2} \times \pi \times (1 \times 10^{-2}\mathrm{cm})^2}{(1.72 \times 1.6 \times 10^{-19}\mathrm{J})} = 4.56 \times 10^8 \tag{7}$$

https://doi.org/10.1021/acsanm.2c01982
ACS Appl. Nano Mater. 2022, 5, 10676−10685

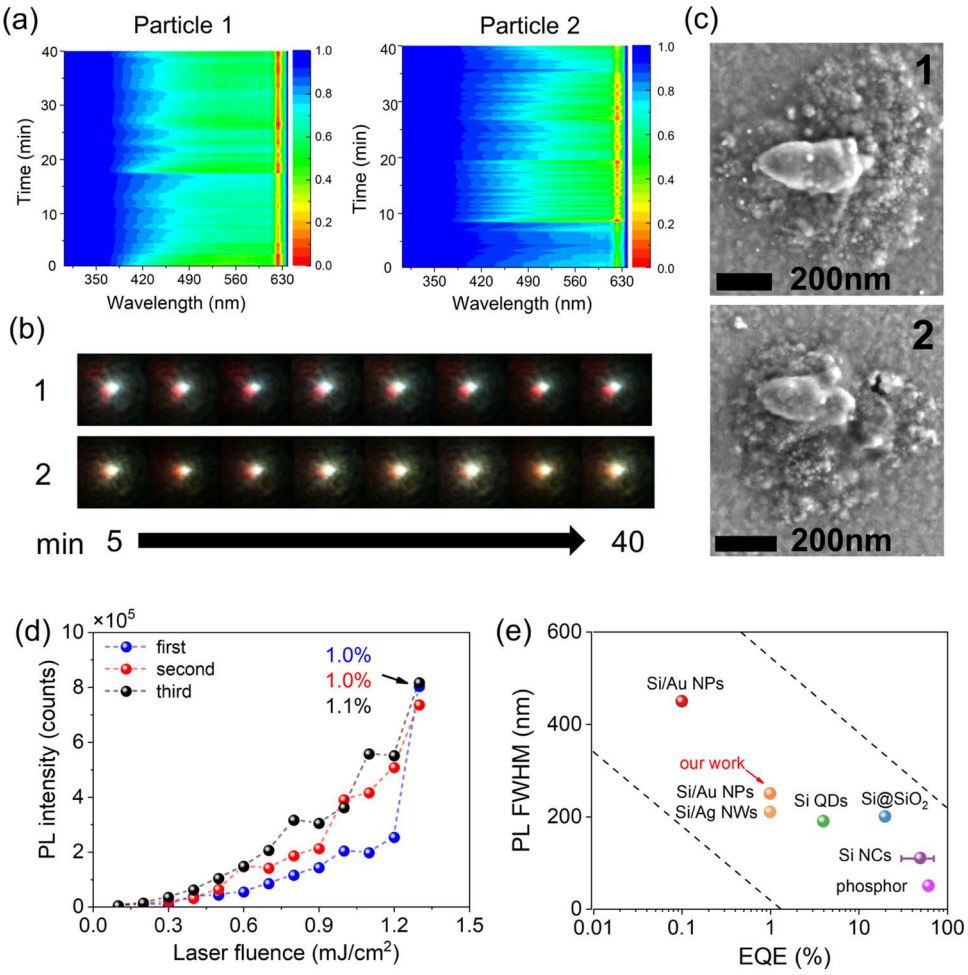

Figure 7. (a) Emission stability tested for two Si/Au nanoparticles. (b) CCD images for the two Si/Au nanoparticles recorded at different times. (c) SEM images for the two Si/Au nanoparticles shown in (a). (d) Dependence of the PL intensity on the laser fluence measured for a Si/Au hybrid nanoparticle for three times. (e) Comparison of the PL bandwidths and quantum efficiencies for Si-related nanoparticles. NPs, NWs, NCs, and QDs are the abbreviations of nanoparticles, nanowires, nanocrystals, and quantum dots.

where w represents laser fluence, s represents laser spot size, $h\nu$ represents single photon energy, $N_2^{ex} = 257$ (see Figure 6b), $r = 0.80$, OD = 2.3×10^{-6}, $g_{ex} = 100$, $\eta_{ex} = 0.80$.[25] Based on the parameters given above, the attenuation coefficient of the optical system was estimated to be $\alpha \sim 3.83 \times 10^{-3}$.

Now we estimate the external quantum efficiencies of the Si/Au nanocavity and the Si/Au nanoparticle shown in Figure 6b,c by using the method described above. The quantum efficiency of Au/Si nanocavity is found to be ~0.4% before the luminescence burst. This value is increased to ~2.4% when the Si/Au nanocavity is lighted up. In contrast, the quantum efficiency of the Si/Au nanoparticle is derived to be ~0.5% below the threshold. It is enhanced to ~1.0% after the luminescence burst. It means that the quantum efficiency of Si/Au nanocavities is larger than that of Si/Au hybrid nanoparticles owing to the existence of optical resonances at which both the absorption and the emission can be enhanced. Physically, the enhancement in the quantum efficiency originates mainly from the injection of high-density electron−hole pairs, which modifies the carrier dynamics via the Auger effect, by exploiting the optical resonances of Si/Au nanocavities.[25] Therefore, the carrier density generated in the Si nanoparticle is the key for enhancing the quantum efficiency. Owing to the absence of optical resonance at ~400 nm, an enhanced quantum efficiency is not observed by using one-photon excitation with 400-nm femtosecond laser pulses.

Actually, the optical resonances of Si/Au nanocavities play a crucial role in determining the threshold for luminescence burst and the quantum efficiency. It is because that the high-density carrier can be generated by resonantly exciting the optical resonance, modifying significantly the carrier dynamics in Si nanoparticles. Basically, the optical resonances of a Si/Au nanocavity are quite sensitive to the dielectric environment. The change in the dielectric environment will lead to the shift and degradation of the optical resonances, which in turn influence the nonlinear optical absorption. As a result, the threshold for PL burst and the quantum efficiency will be modified. In comparison, it is expected that the influence on the PL burst and quantum efficiency of Si/Au nanoparticles will be much smaller because their optical resonances are significantly broadened. This is one of the advantages of Si/Au nanoparticles as compared with Si/Au nanocavities.

We examine the stability of the white light emission from Si/Au nanoparticles. A typical example is shown in Figure 7a where the evolution of the PL spectra of two Si/Au nanoparticles with time is presented. It can be seen that the nonlinear optical emissions from the two Si/Au nanoparticles under the excitation of femtosecond laser pulses are quite

https://doi.org/10.1021/acsanm.2c01982
ACS Appl. Nano Mater. 2022, 5, 10676−10685

stable. The stable white light emission is also reflected in the CCD images recorded at different times, as shown in Figure 7b. In Figure 7c, we show the SEM images of the two Si/Au nanoparticles after the stability test experiments. It is noticed that the morphologies of the Si/Au nanoparticles remain almost unchanged after the long-time excitation. The quantum efficiencies of several Si/Au nanoparticles with different morphologies are also examined. It was found that the quantum efficiencies of these Si/Au nanoparticles are close to ∼1.0% after the luminescence burst. For each Si/Au nanoparticle, the measured quantum efficiency remains almost unchanged after repeated luminescence burst processes, implying the good stability of such white light sources. A typical example is shown in Figure 7d. Moreover, we also found similar luminescence decays for different Si/Au nanoparticles, which exhibit a fast decay with a lifetime of ∼0.13 ns and a slow one with a lifetime of ∼1.00 ns.

For a Si/Au nanocavity, the luminescence burst is reversible, provided that the laser fluence does not exceed too much the threshold. Otherwise, a Si/Au nanocavity will be changed into a Si/Au nanoparticle. For a Si/Au nanoparticle, the luminescence burst is reversible because the nonlinear optical emission is quite stable. For a Si/Au nanocavity, the threshold for the luminescence burst is determined mainly by the excitation wavelength. The closer the excitation wavelength to the optical resonance, the smaller is the threshold. In comparison, the threshold for the luminescence burst of a Si/Au nanoparticle becomes insensitive to the excitation wavelength because of the significant broadening of the optical resonance. In Figure 7e, we compared the PL bandwidths and quantum efficiencies of Si-related nanoparticles reported in the literatures.[1,22,36−40] It is noticed that the increase of quantum efficiency is generally accompanied with the decrease of PL bandwidth. Although the quantum efficiency of the Si/Au hybrid nanoparticles is not large as compared with other nanoparticles, their broad PL bandwidth implies potential applications in nanoscale white light sources with very good stability.

3. CONCLUSIONS

In summary, we have proposed a simple method to fabricate Si/Au hybrid nanoparticles and characterized their nonlinear optical responses under the excitation of femtosecond laser pulses. We first constructed Si/Au nanocavities by placing Si nanoparticles on a thin Au film (or an Au/SiO_2 substrate) and observed luminescence burst when the excitation irradiance exceeds a threshold. We obtained Si/Au hybrid nanoparticles by increasing the laser fluence above the threshold when both Si nanoparticles and Au film are damaged. Luminescence burst is also observed in Si/Au nanoparticles when the laser fluence is further increased. We compare the nonlinear optical emissions from Si/Au nanocavities and Si/Au nanoparticles. It is found that Si/Au nanoparticles possess smaller quantum efficiencies as compared with Si/Au nanocavities owing to the disappearance of the optical resonances. However, more stable white light emission can be achieved by Si/Au nanoparticles, making them suitable for applications in advanced spectroscopy and imaging. Our findings are helpful for understanding the nonlinear optical emission from semiconductor−metal hybrid nanostructures and useful for designing nanoscale white light sources for practical applications.

4. METHODS

4.1. Fabrication. The Si nanoparticles used in our paper were prepared by femtosecond laser ablation. We used a lens with a focal length of 150 mm to focus 800-nm femtosecond laser light (pulse duration: 90 fs, repetition rate: 1 kHz) on the surface of a Si wafer placed in deionized water. The laser power was increased slowly until a continuous stream of slow bubbles was observed on the surface of the Si wafer through a camera. After 15 min of laser processing, the deionized water solution containing Si nanoparticles was transferred to a 10 mL centrifuge tube and centrifuged at 8000 rmp for 5 min. The intermediate layer of the solution was sonicated for 5 min and dropped onto an Au/SiO_2 substrate. The scattering spectra of the formed Si/Au nanocavities were examined by using a dark-field microscope and Si/Au nanocavities with their MMD modes appearing at ∼720 nm were selected for making Si/Au nanoparticles.

4.2. Characterization. A dark-field microscope (Observer A1, Zeiss) equipped with an external broadband light source was utilized to measure the forward scattering spectrum of Si nanoparticles. The 720-nm laser (130 fs, 76 MHz) was imported into an inverted microscope (Observer A1, Zeiss) and focused on the nanoparticles by exploiting an oil objective (100×). The excitation irradiance (or laser fluence) was adjusted by using an optical attenuator inserted in the optical path. The hot electron luminescence emitted from Si/Au nanocavities and Si/Au nanoparticles and the excitation laser light reflected from the substrate were gathered by the same objective and detected by a spectrometer (SR500, Andor).

AUTHOR INFORMATION

Corresponding Author

Sheng Lan − *Guangdong Provincial Key Laboratory of Nanophotonic Functional Materials and Devices, School of Information and Optoelectronic Science and Engineering, South China Normal University, Guangzhou 510006, China;* orcid.org/0000-0002-7277-0042; Email: slan@scnu.edu.cn

Authors

Xiaobing He − *Guangdong Provincial Key Laboratory of Nanophotonic Functional Materials and Devices, School of Information and Optoelectronic Science and Engineering, South China Normal University, Guangzhou 510006, China;* orcid.org/0000-0002-5288-4894

ShiMei Liu − *Guangdong Provincial Key Laboratory of Nanophotonic Functional Materials and Devices, School of Information and Optoelectronic Science and Engineering, South China Normal University, Guangzhou 510006, China*

Shulei Li − *Guangdong Provincial Key Laboratory of Nanophotonic Functional Materials and Devices, School of Information and Optoelectronic Science and Engineering, South China Normal University, Guangzhou 510006, China*

Mingcheng Panmai − *Guangdong Provincial Key Laboratory of Nanophotonic Functional Materials and Devices, School of Information and Optoelectronic Science and Engineering, South China Normal University, Guangzhou 510006, China*

Complete contact information is available at: https://pubs.acs.org/10.1021/acsanm.2c01982

Author Contributions

S.L. and X.H. conceived the idea. S.L., S.L., and M.P. carried out the optical measurements. S.L. and X.H. analyzed the data and wrote the manuscript. S.L. supervised the project. All the authors read and commented on the manuscript.

Notes

The authors declare no competing financial interest.

https://doi.org/10.1021/acsanm.2c01982
ACS Appl. Nano Mater. 2022, 5, 10676−10685

■ ACKNOWLEDGMENTS

This work was financially supported by the National Natural Science Foundation of China (Grant Nos. 11674110 and 11874020) and the Natural Science Foundation of Guangdong Province, China (Grant Nos. 2016A030308010).

■ REFERENCES

(1) Makarov, S. V.; Sinev, I. S.; Milichko, V. A.; Komissarenko, F. E.; Zuev, D. A.; Ushakova, E. V.; Mukhin, I. S.; Yu, Y. F.; Kuznetsov, A. I.; Belov, P. A.; Iorsh, I. V.; Poddubny, A. N.; Samusev, A. K.; Kivshar, Y. S. Nanoscale Generation of White Light for Ultrabroadband Nanospectroscopy. *Nano Lett.* **2018**, *18*, 535−539.

(2) Wang, X.; Wang, M.; Yao, L.; Zhang, L.; Ni, Y.; Xiao, L.; Han, J.-B. A low-cost broadband light source from Au nanorods used for micro-spectroscopy. *J. Lumin.* **2019**, *215*, No. 116637.

(3) Yadav, R.; Arata, H.; Umakoshi, T.; Verma, P. Plasmon nanofocusing for the suppression of photodegradation in fluorescence imaging using near-field scanning optical microscopy. *Opt. Commun.* **2021**, *497*, No. 127206.

(4) Beversluis, M. R.; Bouhelier, A.; Novotny, L. Continuum generation from single gold nanostructures through near-field mediated intraband transitions. *Phys. Rev. B* **2003**, *68*, No. 115433.

(5) Biagioni, P.; Celebrano, M.; Savoini, M.; Grancini, G.; Brida, D.; Mátéfi-Tempfli, S.; Mátéfi-Tempfli, M.; Duò, L.; Hecht, B.; Cerullo, G.; Finazzi, M. Dependence of the two-photon photoluminescence yield of gold nanostructures on the laser pulse duration. *Phys. Rev. B* **2009**, *80*, No. 045411.

(6) Dai, Q.; Ouyang, M.; Yuan, W.; Li, J.; Guo, B.; Lan, S.; Liu, S.; Zhang, Q.; Lu, G.; Tie, S.; Deng, H.; Xu, Y.; Gu, M. Encoding Random Hot Spots of a Volume Gold Nanorod Assembly for Ultralow Energy Memory. *Adv. Mater.* **2017**, *29*, No. 1701918.

(7) Mertens, J.; Kleemann, M. E.; Chikkaraddy, R.; Narang, P.; Baumberg, J. J. How Light Is Emitted by Plasmonic Metals. *Nano Lett.* **2017**, *17*, 2568−2574.

(8) Roloff, L.; Klemm, P.; Gronwald, I.; Huber, R.; Lupton, J. M.; Bange, S. Light Emission from Gold Nanoparticles under Ultrafast Near-Infrared Excitation: Thermal Radiation, Inelastic Light Scattering, or Multiphoton Luminescence? *Nano Lett.* **2017**, *17*, 7914−7919.

(9) Boyd, G. T.; Yu, Z. H.; Shen, Y. R. Photoinduced luminescence from the noble metals and its enhancement on roughened surfaces. *Phys. Rev. B: Condens. Matter* **1986**, *33*, 7923−7936.

(10) Xiang, J.; Chen, J.; Dai, Q.; Tie, S.; Lan, S.; Miroshnichenko, A. E. Modifying Mie Resonances and Carrier Dynamics of Silicon Nanoparticles by Dense Electron-Hole Plasmas. *Phy. Rev. Appl.* **2020**, *13*, No. 014003.

(11) Xiang, J.; Jiang, S.; Chen, J.; Li, J.; Dai, Q.; Zhang, C.; Xu, Y.; Tie, S.; Lan, S. Hot-Electron Intraband Luminescence from GaAs Nanospheres Mediated by Magnetic Dipole Resonances. *Nano Lett.* **2017**, *17*, 4853−4859.

(12) Zhang, C.; Xu, Y.; Liu, J.; Li, J.; Xiang, J.; Li, H.; Li, J.; Dai, Q.; Lan, S.; Miroshnichenko, A. E. Lighting up silicon nanoparticles with Mie resonances. *Nat. Commun.* **2018**, *9*, 2964.

(13) Lin, K.-Q.; Yi, J.; Hu, S.; Sun, J.-J.; Zheng, J.-T.; Wang, X.; Ren, B. Intraband Hot-Electron Photoluminescence from Single Silver Nanorods. *ACS Photonics* **2016**, *3*, 1248−1255.

(14) Huang, J.; Wang, W.; Murphy, C. J.; Cahill, D. G. Resonant secondary light emission from plasmonic Au nanostructures at high electron temperatures created by pulsed-laser excitation. *Proc. Natl. Acad. Sci. U. S. A.* **2014**, *111*, 906−911.

(15) Roura, P.; Costa, J.; López-de Miguel, M.; Garrido, B.; Fort, J.; Morante, J. R.; Bertran, E. Black-body emission from nanostructured materials. *J. Lumin.* **1998**, *80*, 519−522.

(16) Greffet, J.-J.; Bouchon, P.; Brucoli, G.; Marquier, F. Light Emission by Nonequilibrium Bodies: Local Kirchhoff Law. *Phys. Rev. X* **2018**, *8*, No. 021008.

(17) Klaers, J.; Schmitt, J.; Vewinger, F.; Weitz, M. Bose-Einstein condensation of photons in an optical microcavity. *Nature* **2010**, *468*, 545−548.

(18) Haug, T.; Klemm, P.; Bange, S.; Lupton, J. M. Hot-Electron Intraband Luminescence from Single Hot Spots in Noble-Metal Nanoparticle Films. *Phys. Rev. Lett.* **2015**, *115*, No. 067403.

(19) Aspetti, C. O.; Agarwal, R. Tailoring the Spectroscopic Properties of Semiconductor Nanowires via Surface-Plasmon-Based Optical Engineering. *J. Phys. Chem. Lett.* **2014**, *5*, 3768−3780.

(20) Oulton, R. F.; Sorger, V. J.; Zentgraf, T.; Ma, R. M.; Gladden, C.; Dai, L.; Bartal, G.; Zhang, X. Plasmon lasers at deep subwavelength scale. *Nature* **2009**, *461*, 629−632.

(21) Feng, T.; Zhang, W.; Liang, Z.; Xu, Y.; Miroshnichenko, A. E. Isotropic Magnetic Purcell Effect. *ACS Photonics* **2017**, *5*, 678−683.

(22) Cho, C. H.; Aspetti, C. O.; Park, J.; Agarwal, R. Silicon coupled with plasmon nanocavity generates bright visible hot-luminescence. *Nat. Photonics* **2013**, *7*, 285−289.

(23) Glassner, S.; Keshmiri, H.; Hill, D. J.; Cahoon, J. F.; Fernandez, B.; den Hertog, M. I.; Lugstein, A. Tuning Electroluminescence from a Plasmonic Cavity-Coupled Silicon Light Source. *Nano Lett.* **2018**, *18*, 7230−7237.

(24) Mu, Z.; Yu, H.; Zhang, M.; Wu, A.; Qi, G.; Chu, P. K.; An, Z.; Di, Z.; Wang, X. Multiband Hot Photoluminescence from Nanocavity-Embedded Silicon Nanowire Arrays with Tunable Wavelength. *Nano Lett.* **2017**, *17*, 1552−1558.

(25) Xiang, J.; Panmai, M.; Bai, S.; Ren, Y.; Li, G. C.; Li, S.; Liu, J.; Li, J.; Zeng, M.; She, J.; Xu, Y.; Lan, S. Crystalline Silicon White Light Sources Driven by Optical Resonances. *Nano Lett.* **2021**, *21*, 2397−2405.

(26) Li, H.; Xu, Y.; Xiang, J.; Li, X. F.; Zhang, C. Y.; Tie, S. L.; Lan, S. Exploiting the interaction between a semiconductor nanosphere and a thin metal film for nanoscale plasmonic devices. *Nanoscale* **2016**, *8*, 18963−18971.

(27) Sugimoto, H.; Fujii, M. Broadband Dielectric−Metal Hybrid Nanoantenna: Silicon Nanoparticle on a Mirror. *ACS Photonics* **2018**, *5*, 1986−1993.

(28) Zuev, D. A.; Makarov, S. V.; Mukhin, I. S.; Milichko, V. A.; Starikov, S. V.; Morozov, I. A.; Shishkin, I. I.; Krasnok, A. E.; Belov, P. A. Fabrication of Hybrid Nanostructures via Nanoscale Laser-Induced Reshaping for Advanced Light Manipulation. *Adv. Mater.* **2016**, *28*, 3087−3093.

(29) Larin, A.; Ageev, E.; Shiker, A.; Nomine, A.; Makarov, S.; Zuev, D. Nonlinear optical properties of Sponge Si/Au nanoparticle. *J. Phys.: Conf. Ser.* **2020**, *1461*, No. 012081.

(30) Larin, A. O.; Nominé, A.; Ageev, E. I.; Ghanbaja, J.; Kolotova, L. N.; Starikov, S. V.; Bruyère, S.; Belmonte, T.; Makarov, S. V.; Zuev, D. A. Plasmonic nanosponges filled with silicon for enhanced white light emission. *Nanoscale* **2020**, *12*, 1013−1021.

(31) Dmitriev, P. A.; Makarov, S. V.; Milichko, V. A.; Mukhin, I. S.; Gudovskikh, A. S.; Sitnikova, A. A.; Samusev, A. K.; Krasnok, A. E.; Belov, P. A. Laser fabrication of crystalline silicon nanoresonators from an amorphous film for low-loss all-dielectric nanophotonics. *Nanoscale* **2016**, *8*, 5043−5048.

(32) Pang, C.; Li, R.; Zhang, Y.; Li, Z.; Dong, N.; Wu, L.; Yu, H.; Wang, J.; Ren, F.; Chen, F. Tailoring optical nonlinearities of $LiNbO_3$ crystals by plasmonic silver nanoparticles for broadband saturable absorbers. *Opt. Express* **2018**, *26*, 31276−31289.

(33) Sauerbeck, C.; Haderlein, M.; Schürer, B.; Braunschweig, B.; Peukert, W.; Klupp Taylor, R. N. Shedding light on the growth of gold nanoshells. *ACS Nano* **2014**, *8*, 3088−3096.

(34) Zhang, Y.; Grady, N. K.; Ayala-Orozco, C.; Halas, N. J. Three-dimensional nanostructures as highly efficient generators of second harmonic light. *Nano Lett.* **2011**, *11*, 5519−5523.

(35) Liu, Y.; Hu, J.; Yu, X.; Xu, X.; Gao, Y.; Li, H.; Liang, F. Preparation of Janus-type catalysts and their catalytic performance at emulsion interface. *J. Colloid Interface Sci.* **2017**, *490*, 357−364.

(36) Dohnalová, K.; Poddubny, A. N.; Prokofiev, A. A.; de Boer, W. D. A. M.; Umesh, C. P.; Paulusse, J. M. J.; Zuilhof, H.; Gregorkiewicz, T. Surface brightens up Si quantum dots: direct bandgap-like size-tunable emission. *Light: Sci. Appl.* **2013**, *2*, e47.

https://doi.org/10.1021/acsanm.2c01982
ACS Appl. Nano Mater. 2022, 5, 10676−10685

(37) Joo, J.; Cruz, J. F.; Vijayakumar, S.; Grondek, J.; Sailor, M. J. Photoluminescent Porous Si/SiO_2 Core/Shell Nanoparticles Prepared by Borate Oxidation. *Adv. Funct. Mater.* **2014**, *24*, 5688−5694.
(38) Trinh, M. T.; Limpens, R.; Gregorkiewicz, T. Experimental Investigations and Modeling of Auger Recombination in Silicon Nanocrystals. *J. Phys. Chem. C* **2013**, *117*, 5963−5968.
(39) You, C.-Y.; Lin, L.-H.; Wang, J.-Y.; Zhang, F.-L.; Radjenovic, P. M.; Yang, Z.-L.; Tian, Z.-Q.; Li, J.-F. Plasmon-Enhanced Fluorescence of Phosphors Using Shell-Isolated Nanoparticles for Display Technologies. *ACS Appl. Nano Mater.* **2020**, *3*, 5846−5854.
(40) Sangghaleh, F.; Sychugov, I.; Yang, Z.; Veinot, J. G. C.; Linnros, J. Near-unity internal quantum efficiency of luminescent silicon nanocrystals with ligand passivation. *ACS Nano* **2015**, *9*, 7097−7104.

https://doi.org/10.1021/acsanm.2c01982
ACS Appl. Nano Mater. 2022, 5, 10676−10685